



Fabrication and evaluation of SiC/Cu functionally graded material used for plasma facing components in a fusion reactor

Yun-Han Ling^{a,b,*}, Jiang-Tao Li^b, Chang-Chun Ge^b, Xin-De Bai^a

^a Department of Materials Science and Engineering, Tsinghua University, Beijing 100084, People's Republic of China

^b Laboratory of Special Ceramics and Powder Metallurgy, University of Science and Technology Beijing, Beijing 100083, People's Republic of China

Received 23 March 2001; accepted 31 January 2002

Abstract

A new SiC/Cu functionally graded material that contains a spectrum of 0–100% compositional distributions of SiC used for plasma facing component was proposed and fabricated by a novel process termed graded sintering under ultra-high pressure, by which a near dense graded composite has been successfully obtained. Tests on plasma relevant performances showed that in SiC/Cu graded composite the CD₄ production due to chemical sputtering is 85% lower than that of SMF800 nuclear graphite, while its thermal desorption is about 10% of that graphite; fatigue cracks and chemical decomposition were found on the surface of SiC/Cu FGM after 300 cyclic impacts of laser pulse with power density of 398 MW/m²; slight damage was also observed on the material surface after in situ plasma irradiation in a Tokamak facility. © 2002 Elsevier Science B.V. All rights reserved.

PACS: 81.05.Zx; 81.20.Ev

1. Introduction

Graphite material possesses excellent thermal conductivity, stability under high temperature and resistance against irradiation so it has been widely used as plasma facing components (PFCs) in current Tokamak facilities. But its high tritium retention, high chemical sputtering yield and irradiation-enhanced sublimation cause serious carbon contamination to plasma [1]. To reduce the impurities from first wall materials is becoming a realistic issue. Siliconization and boronization with Si- and B-containing organic compounds and helium through in situ glow discharge in Tokamak facili-

ties resulting in Si- and B-based films can effectively reduce the contamination of light impurities in plasma [2–4], but the thickness is limited only within the range of 700–1000 Å. Its lifetime can only survive 140–200 times of discharge so that this kind of film is ineffective for high heat flux components (such as divertor), as the film will be too rapidly eroded in plasma exposure.

As low atomic number (low *Z*) materials, SiC ceramic has a series of advantages for using in fusion reactor, such as good high temperature properties, corrosion resistance, low density, and especially its environmentally benign property for low induced radioactivity after neutron irradiation [5–9]. As it is widely known that metallic copper has better thermal conductivity and machinability than those of graphite; in addition, it is also a kind of metal without hydrogen embrittlement. If a new material integrates both advantages of SiC and copper, it would incorporate properties of high heat corrosion and thermal shock resistance and

* Corresponding author. Address: Department of Materials Science and Engineering, Tsinghua University, Beijing 100084, People's Republic of China.

E-mail address: yunhanling@sina.com.cn (Y.-H. Ling).

will be a promising PFC candidate for future use in thermo-nuclear fusion devices. Nevertheless, cracks or even exfoliations induced by large thermal stress concentration at the interface of SiC and copper may occur on the service condition due to their mismatch of the coefficients of thermal expansion (CTE, at room temperature their difference is about $12.3 \times 10^{-6} \text{ K}^{-1}$).

Japanese scientists firstly proposed the concept of functionally graded material (FGM) [10]. Inhomogeneous materials with gradually changed compositions and structures were made through continuously changing the compositions and structures of two materials with different properties in order that the thermal stress caused by the mismatch of CTEs at the interfaces can be reduced and thus the cracks and failure can be prevented.

The large melting point difference between SiC and Cu (about 1500 K) and no overlap of sintering temperature ranges make it difficult to fabricate a full compositional distribution (from 0% to 100%) SiC/Cu FGM even by delicate conventional processes [11,12], and SiC/metal graded composite was thought to be eliminated from consideration through simultaneous sintering [13].

In this paper, the idea of FGM was adopted and a new approach for fabricating SiC/Cu FGM, which has a characteristic of distinct resistivity and melting point discrepancy and thereby rapid graded sintering under ultra-high pressure (GSUHP), was exploited. A preliminary evaluation of its plasma-relevant performance was conducted.

2. Experimental procedures

In view of their obvious resistivity gap between SiC and Cu, it can be expected that a gradual resistance distribution and thus a escalated power and temperature profile will be established along copper layer, ceramic-dispersed copper rich layer, percolation layer, copper-dispersed ceramics rich layer and pure ceramics layer when a strong current passing through SiC/Cu FGM sample. The temperature difference between graded layers to copper layer ($T_{\text{grad}} - T_{\text{cu}}$) can be simply deduced by Fourier's heat conduction law and it was approximately proportional to the square of FGM thickness and current density applied [14]. By adjusting the inherent resistance of FGM and external electric current input, graded sintering of SiC/Cu FGM, which has a characteristic of high melting point difference, may be realized. However, ultra-high pressure is a necessity to shorten sintering time and subsequently prevent macro diffusion between copper and ceramics.

The experimental setup is schematically illustrated in Fig. 1. This device consisted of a mechanical press, and associated electrical and hydraulic systems. A FGM

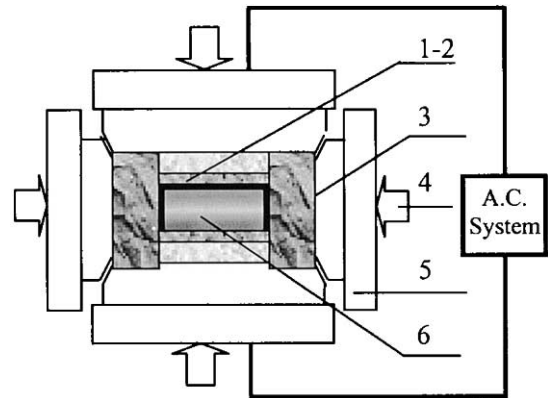


Fig. 1. Schematic illustration of experimental setup: (1) steel platelet; (2) graphite platelet; (3) pyrophyllite sleeve; (4) pressurized orientation; (5) anvil of WC hard alloy (6) SiC/Cu green compact.

assembly, which contained SiC/Cu FGM green compact, was placed in the pressure vessel. The pressure was applied by raising the bottom anvil with force provided by lower hydraulic ram. The sample assembly was encapsulated in a pyrophyllite sleeve, which was acted as heat/electric insulator in graded sintering. Graphite and steel platelets were used as sealing and pressure-transferring components respectively as well as electric conductor. The alternating current (AC) passed through and the FGM green compact was heated mainly by self-exothermicity and thermal conduction.

Ultra-fine SiC powder with an average particle size of 150 nm and a purity of more than 99%, and Cu powder with a particle size less than $44 \mu\text{m}$ and a purity of more than 99.9% were used. B_4C powder (15 wt%) with a mean particle size of 800 nm and a purity of about 95% was employed as sintering additive to activate the densification of SiC and improve its toughness.

SiC, B_4C and Cu powders were mixed and milled with different volume ratios according to the design of compositional distribution in the graded layers of the FGM [15]: $C = (x/d)^p$, where C is the volume fraction, x the relative distance from the surface, d the thickness of the FGM layer, and p the compositional distribution factor. In this work, experiments on the fully compositional distributions (0–100% SiC) of six-layered SiC/Cu FGM with $p = 0.6, 1.0, 1.4, 1.8$ were conducted. In this paper, the lower p value means less ceramic content in an overall SiC/Cu FGM. The compositional distribution curves of SiC/Cu FGM with different p values are shown in Fig. 2. The powders with different compositions were stacked layer by layer in a steel mould to form a green compact of $\varnothing 20 \text{ mm} \times 10 \text{ mm}$. For samples to investigate the densification of different layers in a FGM, graphite foil of thickness 0.2 mm was introduced at the

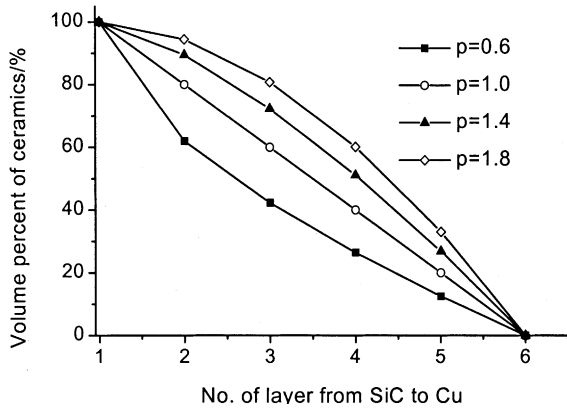


Fig. 2. Compositional distribution curves of SiC/Cu FGM with different p values.

interface of graded layers to separate every layer of SiC/Cu FGM after sintering. Because the thickness of each layer was pre-designed (for example in the paper a six-layered SiC/Cu FGM with dimension of $\varnothing 20 \text{ mm} \times 6 \text{ mm}$, the thickness of each layer is 1 mm), and the volume of ceramic and metal of each layer was distributed by $C = (x/d)^p$, so the mass of ceramics and metal was therefore fixed and the theoretical density of each layer can be easily calculated.

Graded sintering was performed under pressures of 3000–5000 MPa, an electric power input of about 12 kW (7.5 V, 1600 A) and sintering times of 30–60 s.

The density of sintered SiC/Cu FGMs was measured by Archimedes' method after polishing and wax applying. Scanning electron microscopy (SEM) was employed to characterize microstructure. A thermal shock test of SiC/Cu FGMs was performed by cyclic laser pulses and the properties related to plasma were evaluated by in situ irradiation with high-energy deuterium beam.

3. Results and discussion

3.1. Consolidation analysis

When strong current passed through the SiC/Cu FGM green compact, a gradient temperature profile was quickly established, and the highest temperature was located in ceramic side. It is easy to comprehend that the sintering rate of cermet composite is elevated with increasing the content of low melting point metals in homogeneous temperature field. But the sintering characteristics differ from layers in graded temperature zone, lower p value FGM means less ceramics (or more copper) in the overall SiC/Cu FGM, and therefore has better densification, while higher p value FGM has less copper content, it is not easy to sinter ceramics when liquid phase is lack, especially in short time, so different

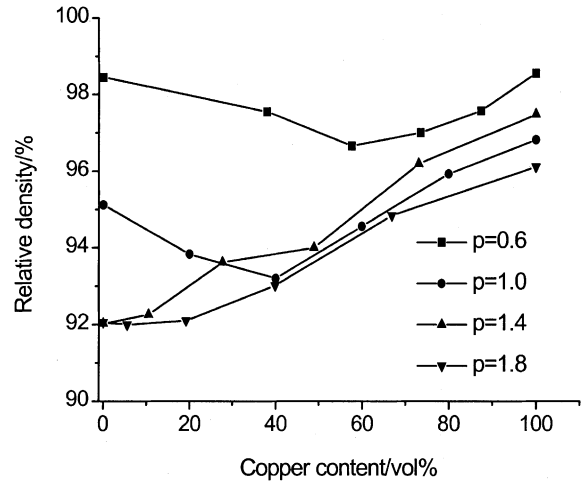


Fig. 3. Effects of copper content on relative density of different layers in SiC/Cu FGM (7.5 V, 1600 A; 5000 MPa; 40 s).

p value FGMs mean different metal contents and thus lead to different densification under the same sinter condition, which is shown in Fig. 3. For $p = 0.6$ and 1.0 of the six-layered SiC/Cu FGMs, the densities of the 3rd (40–60 vol.% Cu, the first layer is pure ceramic) drop compared with their neighboring parts, which might be caused by two paralleling influences. Firstly, the high temperature of ceramic side leads to copper melting or partial evaporation, and thus copper was extruded from ceramic matrix for local overpressure; secondly, the copper phase transition affected the ceramic sintering by absorbing heat and therefore reduced the local temperature of that layer those copper located. Whilst $p > 1.0$, the density of ceramics-rich layer is relatively lower than that of copper-rich layer, which is due to lower Cu content in overall FGM compared with that of $p < 1.0$; besides, the solid state sintering mode of ceramics layer, which is always considered to be time-dependent diffusion, is not beneficial to high consolidation during transient process.

The sintering effect of the whole SiC/Cu FGM was shown in Fig. 4. It is clear that pressure has important and positive influence on the FGMs' densification. This is because the increasing of pressure can accelerate the process of metal creep and liquid phase percolation; and as to ceramic layer, it favors the grain boundary sliding (disintegration or plastic flow) and extrusion creep. However, the densification decreased with the increase of p values for lower copper content in the overall FGMs. For ceramic-rich layers, the driving force of solid state sintering is mainly contributed by the surface energy of ultra-fine ceramic powders. At the final stage, densification's process depends on the vacancy diffusion induced by the curvature difference of sinter neck. Although the diffusion induced by the heating gradient (T_{grad}) is greater than that of conventional hot-pressing

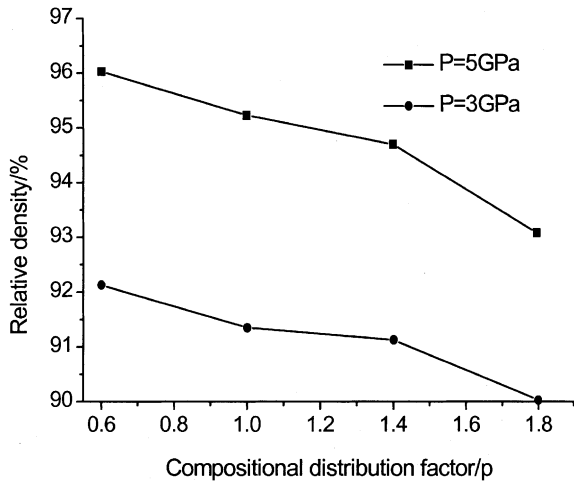


Fig. 4. Relative density as a function of different p values of SiC/Cu FGM (7.5 V, 1600 A; 40 s).

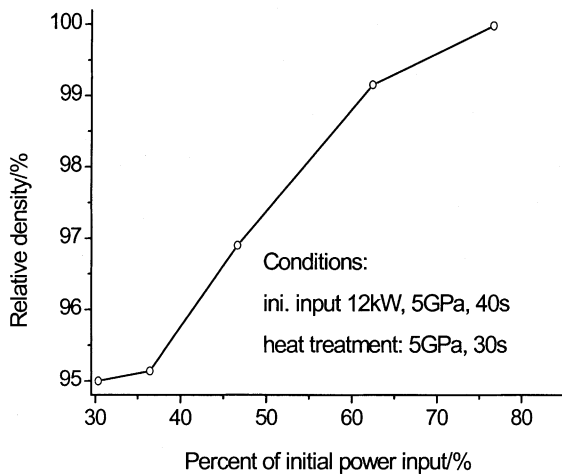


Fig. 5. Effects of power of heat treatment on densification of SiC/Cu FGM with $p = 1.0$.

[16], rapid sintering is not conducive to the removal of pores, especially to higher p value SiC/Cu FGMs.

The influence of post heat treatment on densification of $p = 1.0$ SiC/Cu FGM was illustrated in Fig. 5, it is noticeable that a near dense SiC/Cu FGM has been achieved when a secondary power of 65–80% initial input was applied. Heat treatment can further improve ceramic sintering and promote liquid copper re-infiltrating into ceramic matrix (percolation flow). Nevertheless, it can be reasonably expected that the macroscopically compositional distribution of graded SiC/Cu composite should retain for very short heating duration.

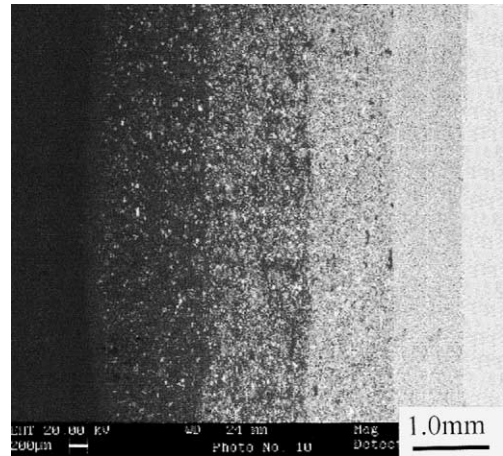


Fig. 6. SEM of overall six-layered SiC/Cu FGM with $p = 1.0$ after heat treatment (Cu contents are 0, 20, 40, 60, 80, 100 vol.%, respectively).

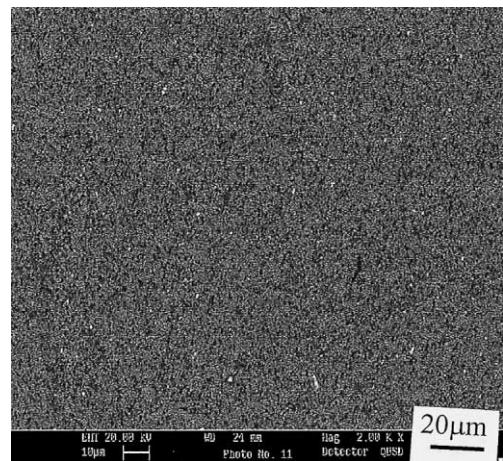


Fig. 7. SEM of pure ceramic layer of SiC/Cu FGM.

3.2. Microstructure investigation

To examine the sintering and heat treatment effects of SiC/Cu FGM, microstructure investigation was indispensable. Fig. 6 presents a backscattering image of the overall six-layered SiC/Cu FGM with $p = 1.0$ after heat treatment. From that pronounced compositional changes were demonstrated, which reflects no macro elemental migration during rapid sintering under ultra-high pressure and subsequent short duration of heat treatment. Fig. 7 depicts microstructure of pure SiC–B₄C ceramics (the top layer) of $p = 1.0$ SiC/Cu FGM, it is obvious that ultra-fine SiC has been sintered and bonded well together, while the additive B₄C or pores were dispersed uniformly among them.

3.3. Chemical sputtering and thermal desorption performances

The chemical sputtering performance of SiC/Cu FGM with $p = 1.0$ after heat treatment was conducted in LAS-2000 apparatus. The sputtering products were measured under irradiation of 3 keV, 4.6×10^{15} D^+ / cm^2 , and the change of ratio SiD_4^+/CD_4^+ with temperature was recorded by mass-spectrometry. In comparison with graphite SMF800, SiC/Cu FGM shows much lower CD_4 production, the peak value of CD_4 production, which reached at 750 K, is about 15% of that graphite SMF800, and the temperature of CD_4 peak value shifts to a lower 30 K, as shown in Fig. 8. The chemical sputtering data imply that the bonding strength of ceramic SiC and its chemical stability against the erosion of deuterium beam are much higher than those of nuclear graphite.

Thermal desorption was performed after sample's mechanical polishing and ultrasonic cleaning. The experimental procedures were: firstly, vacuum degassing for about 2 h at about 1300 K; then, after the temperature of the sample cooled down to room temperature (RT), a deuterium ion with 2.7 keV energy was implanted and the total flux was 1.2×10^{18} ions. At the base pressure 1×10^{-6} Pa, the thermal release spectra were measured by fast temperature rising from RT–1223 K. The results are shown in Figs. 9 and 10, the curve of temperature rise was also drafted in the figures. The CD_4 production of SiC is obviously lower than that of graphite, approximately 10% of that graphite SMF800 and the SiD_4 production is lower than that of CD_4 by at least one order. The peak temperatures of D_2 and CD_4 of SiC are obviously higher than that of graphite, which means the activation energies of desorption for D_2 and

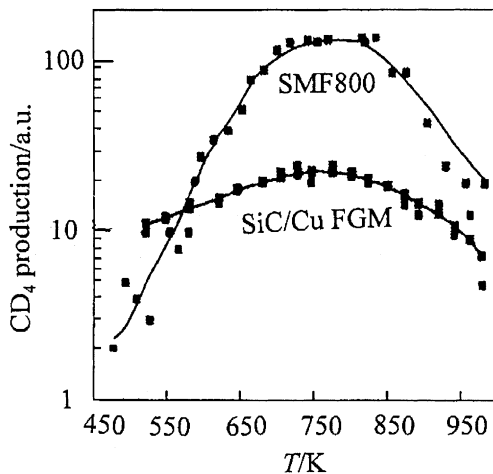


Fig. 8. Temperature dependences of CD_4 products under 3 keV, $4.6E15D^+ s^{-1} cm^2$ irradiation.

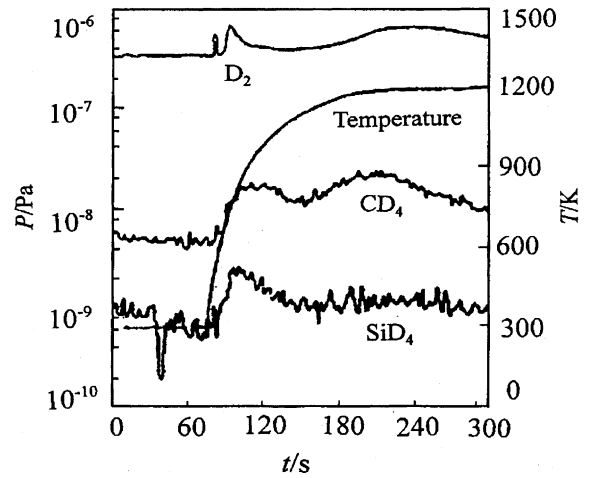


Fig. 9. Spectra of CD_4/SiD_4 thermal desorption of $p = 1.0$ SiC/Cu FGM.

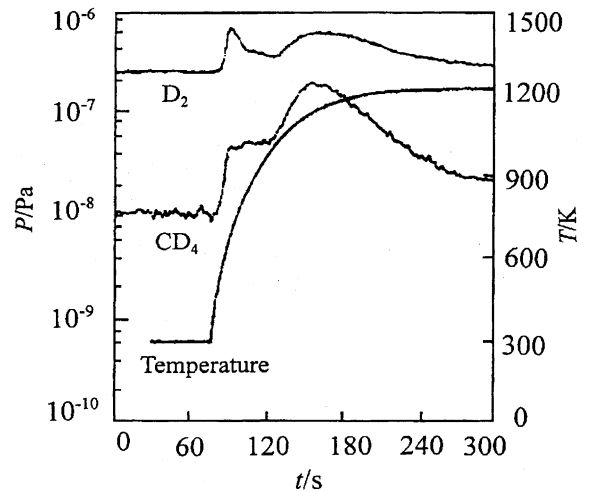


Fig. 10. Spectra of CD_4 thermal desorption of nuclear graphite SMF800.

CD_4 of SiC sample are also higher than those of graphite.

It can be concluded from above results that SiC/Cu FGM has higher chemical sputtering resistance under plasma irradiation than that of nuclear graphite SMF800, and its lower gas desorption compared with nuclear graphite also means lower deuterium retention in D–T reaction and therefore SiC/Cu FGM will be beneficial to the circulation of fuel deuterium in fusion device.

3.4. Hot impact experiment

Hot impact experiment for SiC/Cu FGM was preliminarily performed by high-energy laser pulse; the

experimental parameters are as follows:

Pulse length (t): 4 ms Dot diameter: 0.4 cm
 Energy density: 398 MW/m² Times: 100, 300.

SEM and weight loss examinations were employed to analyze and evaluate the thermal shock behavior of SiC/Cu FGM with $p = 1.0$, such as exfoliation, evaporation, crack and thermal fatigue properties. After 100 and 300 times' impact, the weight loss rates (weight loss/area of laser dot) of SiC/Cu FGM were -11.59 and -44.51 mg/cm², respectively. It is noticeable that the weight losses of FGMs are negative, which means the weights of samples are increasing after laser shocks, and the increase is probably due to oxidation of copper matrix in the air at the temperature rise of whole samples. From the surface of copper, it can be seen clearly that the color has changed into dark red. However, crater-like concavities and cracks were found on SiC surface after laser impact, as shown in Fig. 11. The melting also seemed to occur in the areas. Fig. 12 is the magnification of the surface microstructure of pure ceramic layer of SiC/Cu FGM in the beam spot, where the pits or vacancies seem to be the residual places after volatilization. The small circular dots on the edge of laser spots, which is shown in Fig. 13, contained free Si assayed by SEM building-out energy dispersive spectrometer analysis. As a result, from Figs. 11–13 it can be inferred that chemical decomposition of SiC must have taken place, and the



Fig. 11. Ceramic surface of $p = 1.0$ SiC/Cu FGM after 300 times cyclic hot impact by laser pulse.

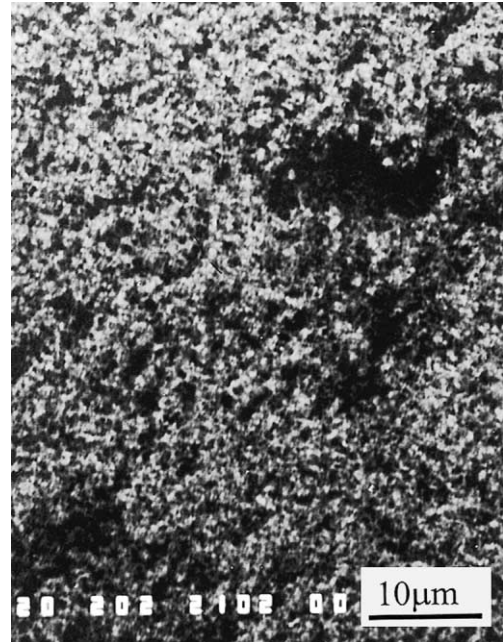


Fig. 12. Microstructure of SiC ceramic layer on the laser beam spot.



Fig. 13. Microstructure of SiC ceramic layer on the edge of beam spot.

evaporation of Si on the laser beam spot should also happen, though its weight loss was less than the weight increase of copper by oxidation. From the information

obtained, it can be inferred that large thermal stress occurred on interface of inside/outside the beam spots under strong heat impact is due to SiC ceramic itself has low thermal conductivity that cannot dissipate concentrated energy, which led to the generation and propagation of cracks. The appearance of free silicon suggested the temperature inside or outside beam spots should exceed 2873 K, the normal decomposition temperature of SiC in air. Qualitatively speaking, the damage mechanisms of SiC/Cu FGM are thermal erosion, cracking, melting or evaporation under 398 MW/m² energy density. The cracking and evaporation may degrade the thermal or mechanical properties of materials, while the latter one may cause weight loss and thus directly reduce the lifetime of materials as PFC on service.

A monolithic hot-pressed SiC ceramic with the same testing dimension of $\varnothing 10 \text{ mm} \times 5 \text{ mm}$ of $p = 1.0$ SiC/Cu FGM was used to simply compare their properties of hot impact resistance. No macro defects (cracks or exfoliations) were observed by naked eyes at the interface of graded layers of SiC/Cu FGM after 100 and 300 cyclic impacts, while monolithic SiC was broken into several pieces after only 20 times of laser shots and therefore no weight loss data was obtained under the same energy density of 398 MW/m². Although more meticulous tests and many details are waited to be explored, the preliminary result indicates that SiC/Cu FGM has much better thermal shock resistance than that of monolithic ceramic SiC.

3.5. Physical sputtering damage-resistant experiment

The plasma physical sputtering damage of the surface of SiC/Cu FGM can represent its physical sputtering performance. Tokamak in situ plasma irradiation experiment was performed in the Chinese HL-1M facility; the discharge parameters are as follows:

Intensity of perpendicular magnetic field: 2 T
 Times: 66
 Toroidal current: 120–200 kA
 Lifetime of plasma: 1.2 s
 Linear mean electron density: $(1\text{--}1.4) \times 10^{13} \text{ cm}^{-3}$
 Peripheral electron density: $(2\text{--}4) \times 10^{12} \text{ cm}^{-3}$
 Peripheral temperature of electron: 100–200 eV.

XRD and SEM were employed to analyze the irradiated samples. Fig. 14 shows the morphologies of irradiated SiC/Cu FGM sample with 80 vol.% SiC on the surface, it is conspicuous that the sample surface was seriously damaged, almost smashed, and the melting of copper was displayed (the globule size). Fig. 15 is the morphology of irradiated $p = 1.0$ SiC/Cu FGM, in which surface contains pure ceramics, only slight cracks were found, which indicates much better sputtering-



Fig. 14. Morphology of 80 vol.% SiC-contained surface of SiC/Cu FGM after in situ plasma irradiation.



Fig. 15. Morphology of SiC/Cu FGM surface after in situ plasma irradiation.

resistant property than that cermet surface of SiC/Cu FGM. XRD results shows no distinct change of crystal structure of SiC, while small increase in peak width in graphite SMF800 specimen, indicating change of crystal

structure and increase of crystal lattice defects; besides, after plasma irradiation, evident characteristics of plasma sputtering damage is noticed in graphite SMF800 [17].

4. Summary

(1) SiC/Cu FGM with compositional spectrum of 0–100% was firstly fabricated by GSUHP.

(2) Pressure and heat treatment have strong influence on the densification of SiC/Cu FGM. A near dense of composite has been obtained on conditions of 5000 MPa applied, 12 kW heating for 40 s and subsequent heat treatment on 65–80% initial power input for 30 s.

(3) Microstructure investigation shows that the graded compositional distribution of SiC/Cu FGM retains after GSUHP.

(4) The chemical sputtering of SiC/Cu FGM is 85% lower than that of nuclear graphite SMF800, and the thermal desorption ratio is about 10% of that graphite.

(5) Cracks appeared on the surface of SiC/Cu FGM after 300 times hot impact with 398 MW/m² energy density applied, and chemical decomposition of SiC were found on laser beam dots. The damage mechanisms of SiC/Cu FGM are thermal erosion and evaporation.

(6) The surface of SiC/Cu FGM presents slight damage after Tokamak in situ plasma irradiation after 66 times discharges.

Acknowledgements

The authors would like to express their thanks for the financial support of China National Committee of High Technology New Materials under grant no. 863-715-011-0230.

References

- [1] V. Barabash, M. Akiba, I. Mazul, et al., *J. Nucl. Mater.* 233–237 (1996) 718.
- [2] C. Garcia-Rosales, E. Gauthier, J. Roth, et al., *J. Nucl. Mater.* 189 (1992) 1.
- [3] C. Mingam, R.W. Conn, F. Dias, et al., *Fusion Technol.* 175 (1990) 424.
- [4] N.M. Zhang, E.Y. Wang, S.J. Qian, et al., *J. Nucl. Mater.* 266–269 (1999) 747.
- [5] S. Sharafat, R.H. Jones, A. Kohyama, et al., *Fusion Eng. Design* 29 (1995) 411.
- [6] A. Donato, R. Andreani, *Fusion Technol.* 26 (1996) 58.
- [7] L.L. Snead, R.H. Jones, A. Kohyama, P. Fenici, *J. Nucl. Mater.* 233–237 (1996) 26.
- [8] P. Fenici, A.J. Rebelo Frias, R.H. Jones, et al., *J. Nucl. Mater.* 258–263 (1998) 215.
- [9] E.E. Bloom, *J. Nucl. Mater.* 258–263 (1998) 257.
- [10] M. Niino, T. Hirai, R. Watanabe, *J. Jpn. Comp. Mater.* 13 (6) (1987) 257.
- [11] P. Czubarow, D. Seyferth, *J. Mater. Sci.* 32 (8) (1997) 2121.
- [12] Y.L. Lee, S.L. Lee, C.L. Chuang, et al., *Powder Metall.* 46 (10) (1998) 3491.
- [13] A. Mortensen, S. Suresh, *Int. Mater. Rev.* 40 (6) (1995) 239.
- [14] Y.H. Ling, C.C. Ge, J.T. Li, C. Huo, *Ceram. Trans.* 114 (2001) 333.
- [15] T. Hirano, J. Teraki, T. Yamada, in: M. Yamanouchi, M. Koizumi, T. Hirai, I. Shiota (Eds.), *Proceedings of 1st International Symposium on Functionally Gradient Materials FGM'90*, Tokyo, Functionally Gradient Materials Forum and The Society of Non-Traditional Technology, 1990, p. 5.
- [16] M.R. Young, M. Reginald, *J. Am. Ceram. Soc.* 72 (6) (1989) 1080.
- [17] C.C. Ge, Y.K. Li, in: *Proceedings of the 5th China–Japan Symposium on Materials in Advanced Energy System and Fission and Fusion Engineering*, Xi'an, China, 26 November, 1998, p. 222.